

Hybrid C60 Fullerene Conjugates as Vectors for DNA Delivery

Cristina M. Uritu[†], Cristian D. Varganici[†], Laura Ursu[†], Adina Coroaba[†], Alina Nicolescu[†], Andrei I. Dascalu[†], Dragos Peptanariu[†], Daniela Stan[‡], Cristina A. Constantinescu[‡], Viorel Simion[‡], Manuela Calin[‡], Stelian S. Maier^{§†}, Mihail Barboiu^{§*}, Mariana Pinteala[†]

[†] “Petru Poni” Institute of Macromolecular Chemistry, Iasi, 700487, Romania

[‡] “Nicolae Simionescu” Institute of Cellular Biology and Pathology, Bucharest, 050568, Romania

[§] “Gheorghe Asachi” Technical University of Iasi, Iasi, 700050, Romania

^{*} Institut Européen des Membranes, ENSCM-UMII-CNRS 5635, 34095, Montpellier, France

Supporting Information

Table of contents

Figure SI-1. Synthesis of C60-PEI conjugate.	S2
Figure SI-2. Synthesis of C60-PEG-PEI conjugate.	S2
Figure SI-3. UV-VIS spectra confirming the advance of conjugation reaction between C60 fullerene and the PEI and PEG precursors.	S3
Figure SI-4. ¹ H-NMR spectrum of branched PEI precursor.	S4
Figure SI-5. ¹³ C-NMR spectrum of branched PEI precursor.	S4
Figure SI-6. ¹ H-NMR spectrum of α -amino-PEG precursor.	S5
Figure SI-7. ¹³ C-NMR spectrum of α -amino-PEG precursor.	S5
Figure SI-8. ¹ H-NMR spectrum of the C60-PEI conjugate.	S6
Figure SI-9. ¹³ C-NMR spectrum of the C60-PEI conjugate.	S6
Figure SI-10. FT-IR spectra of the precursors and C60-based conjugates.	S7
Figure SI-11. The wide scan XPS spectra of PEI, C60-PEI, C60-PEG-PEI, and PEG.	S8
Table SI-1. Elemental composition derived from wide XPS spectra.	S8
Figure SI-12. Comparative thermal characterization of PEI and PEG precursors, and of synthesized C60-PEI and C60-PEG-PEI conjugates.	S9
Figure SI-13. DSC heating curves of precursors and synthesized C60-based conjugates.	S9

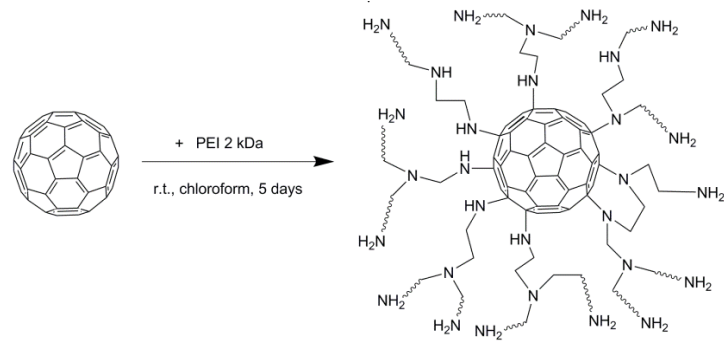


Figure SI-1. Synthesis of C₆₀-PEI conjugate.

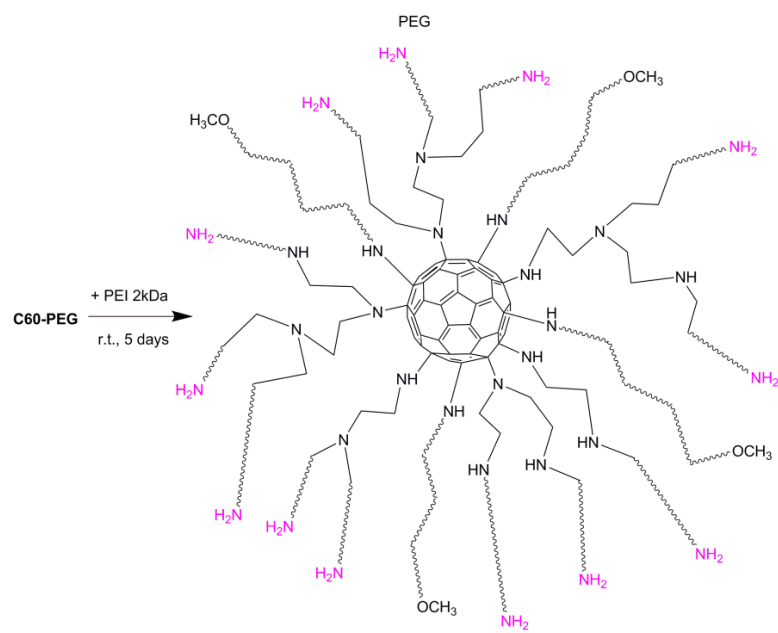
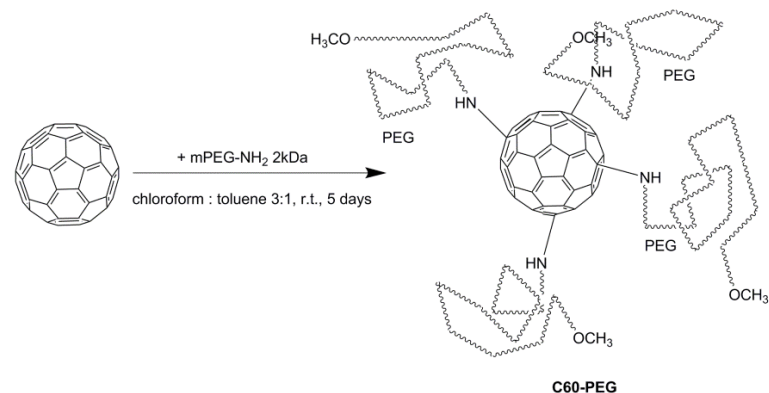


Figure SI-2. Synthesis of C₆₀-PEG-PEI conjugate.

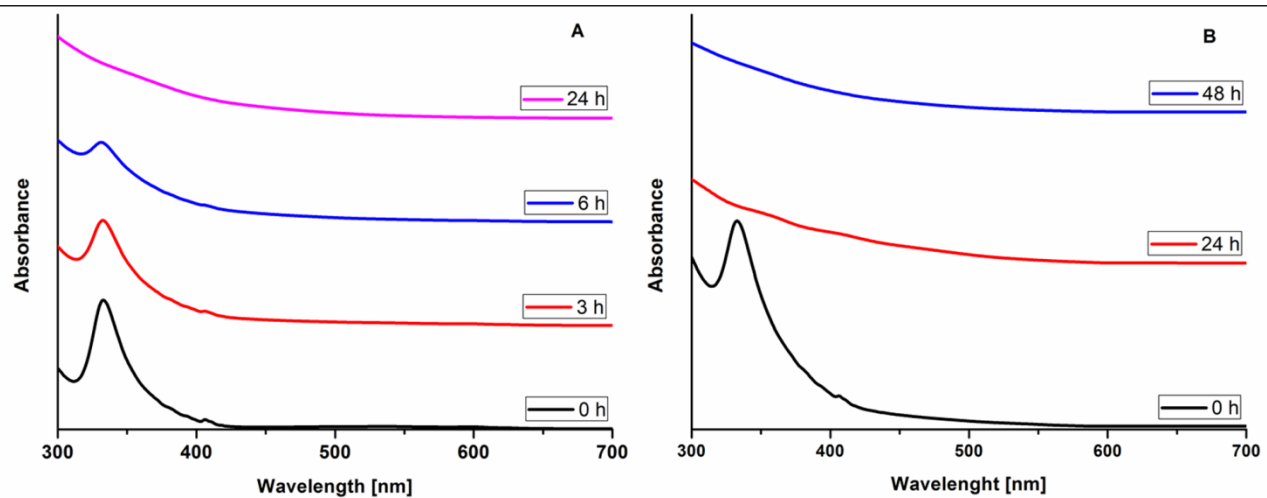


Figure SI-3. UV-VIS spectra confirming the advance of conjugation reaction between C₆₀ fullerene and the PEI and PEG precursors.

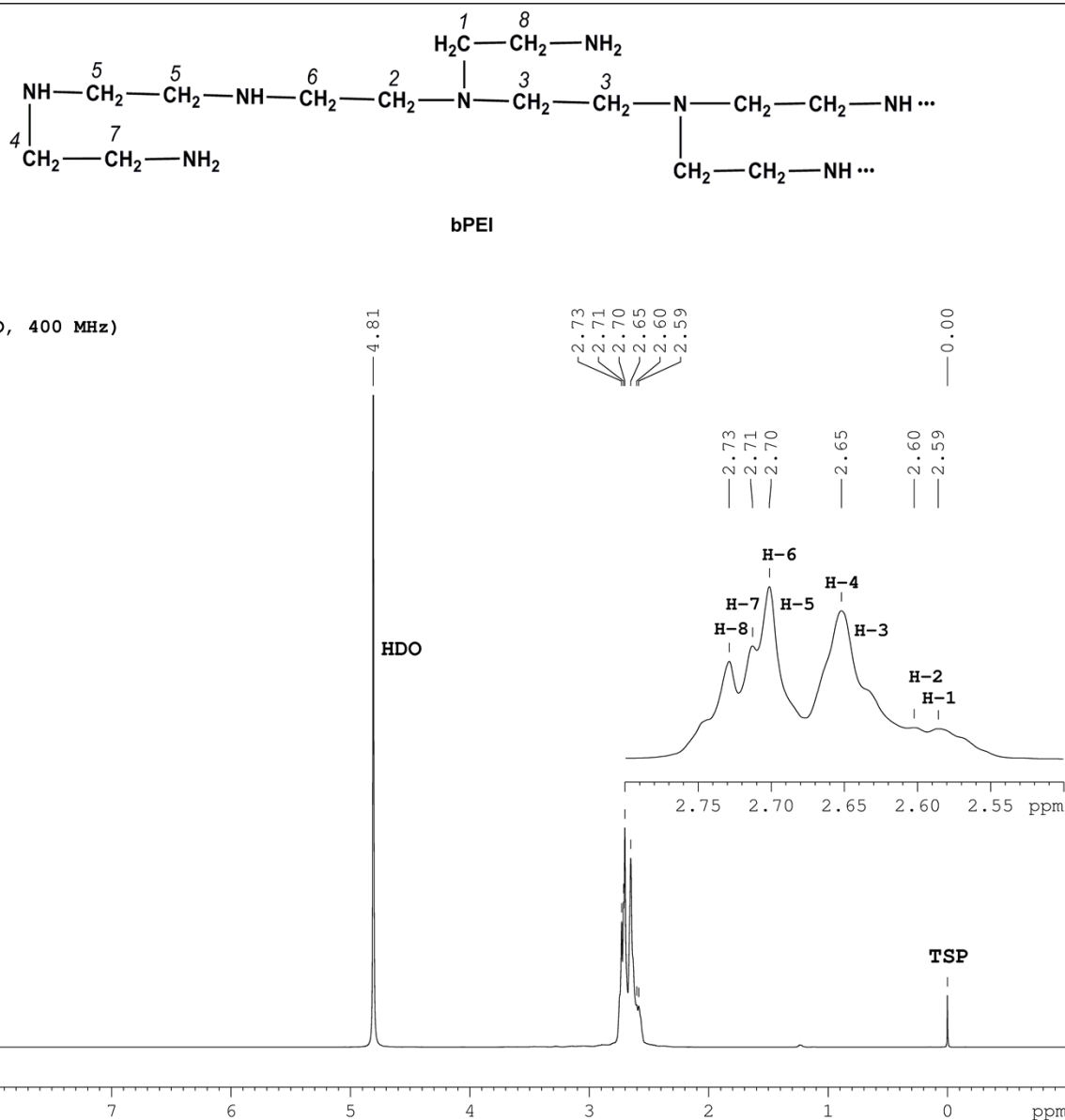
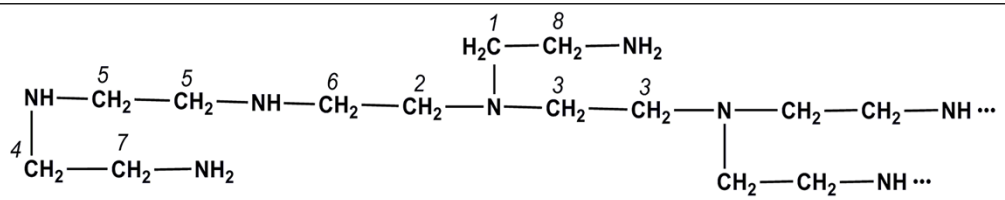


Figure SI-4. ¹H-NMR spectrum of branched PEI precursor.



bPEI

^{13}C NMR (D₂O, 100 MHz)

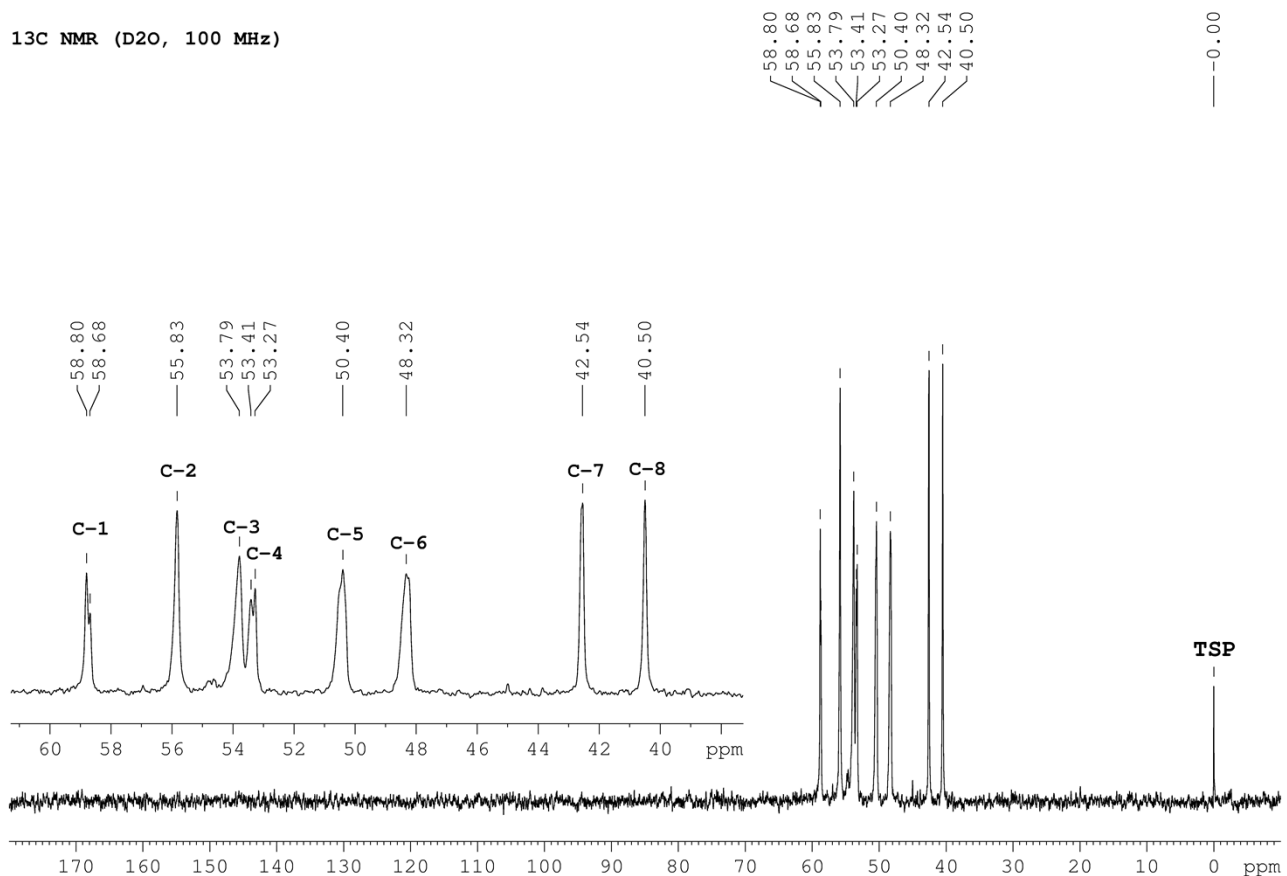
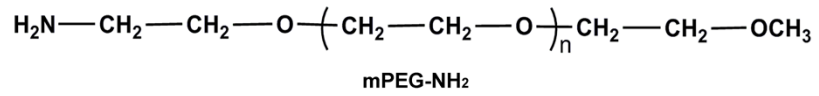


Figure SI-5. ^{13}C -NMR spectrum of branched PEI precursor.



¹H NMR (D₂O, 400 MHz)

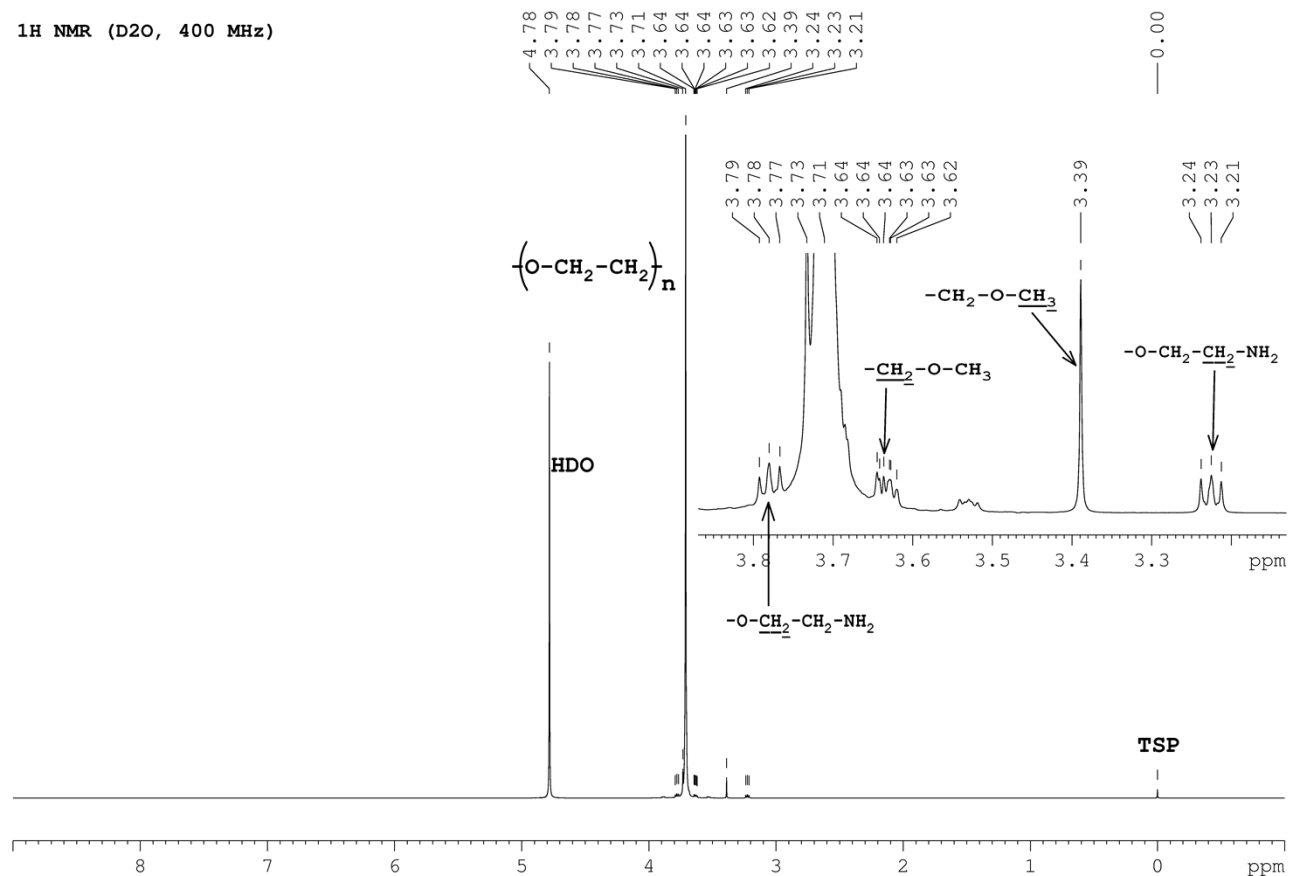


Figure SI-6. ¹H-NMR spectrum of α-amino-PEG precursor.

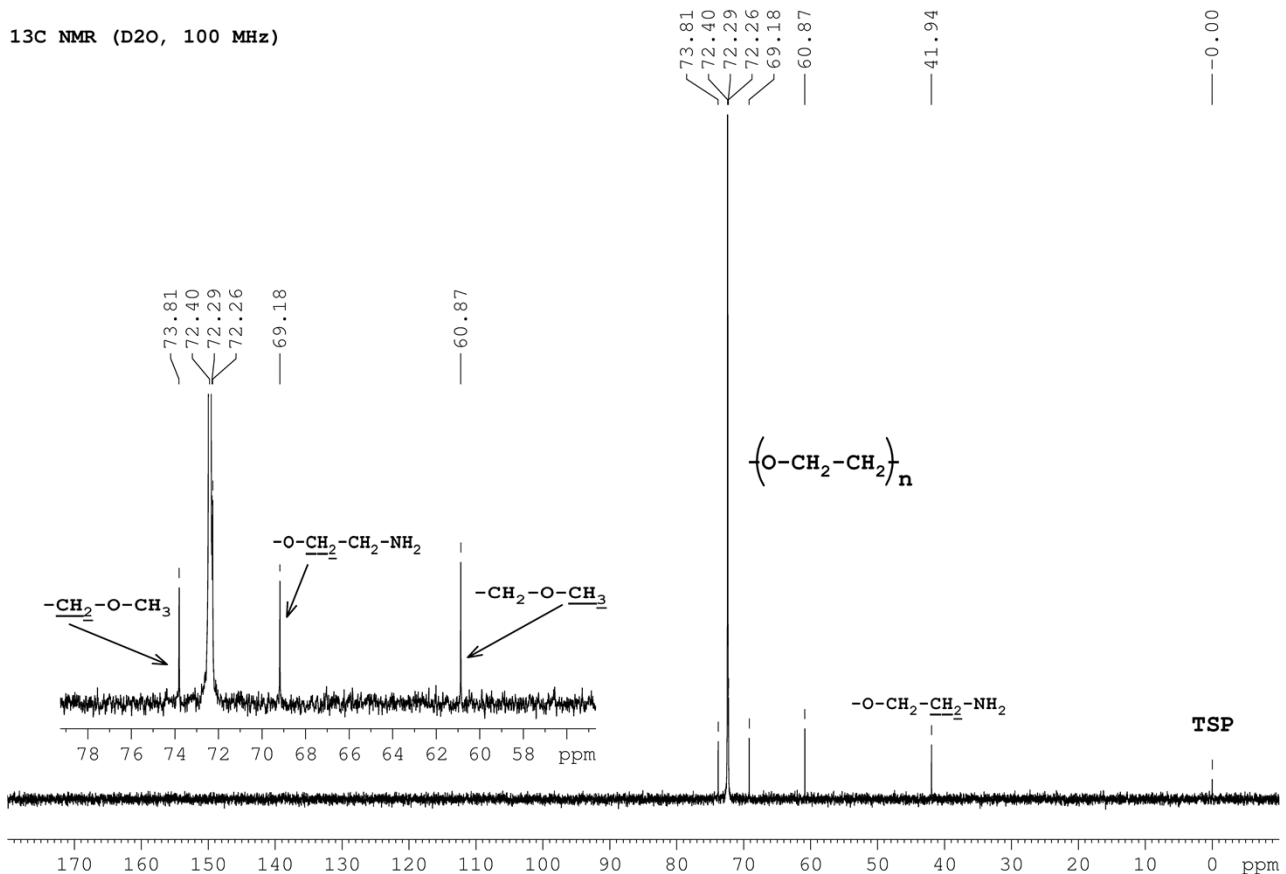
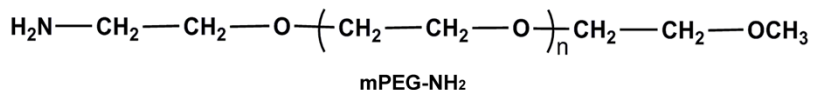
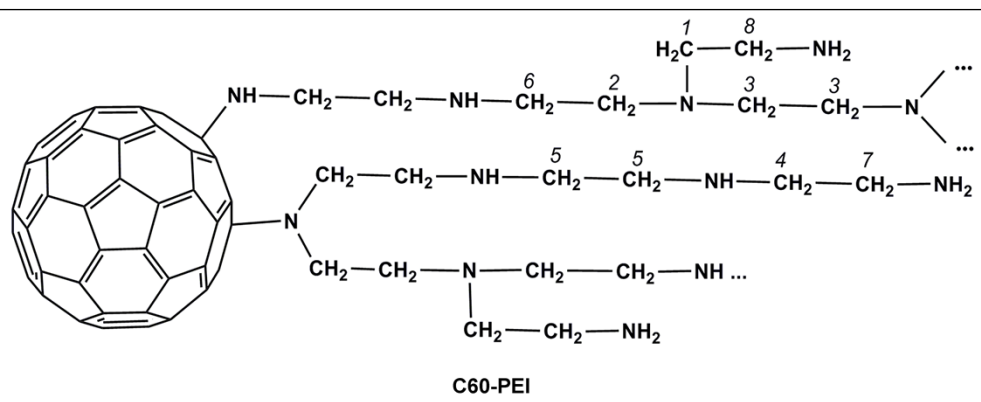


Figure SI-7. ^{13}C -NMR spectrum of α -amino-PEG precursor.



¹H NMR (D₂O, 400 MHz)

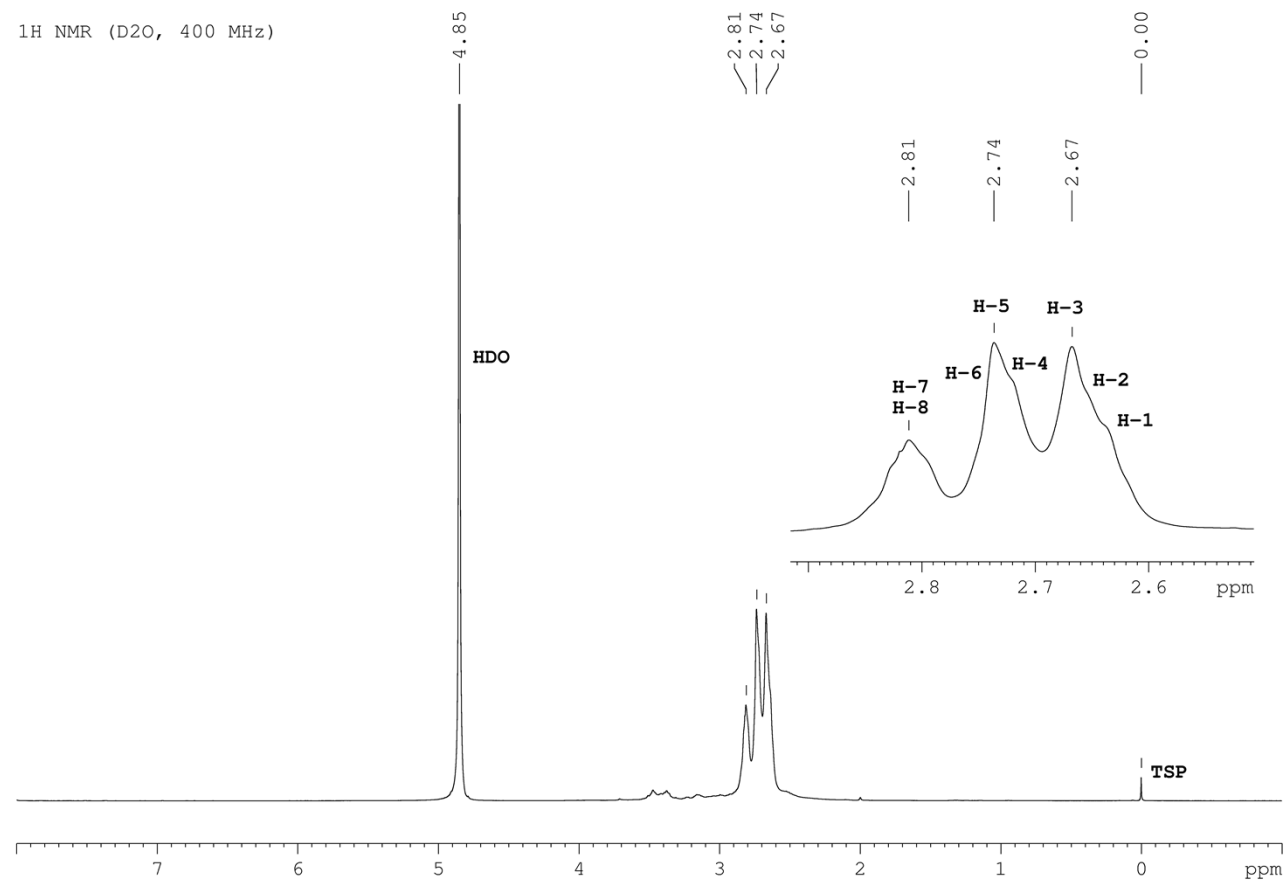


Figure SI-8. ¹H-NMR spectrum of the C60-PEI conjugate.

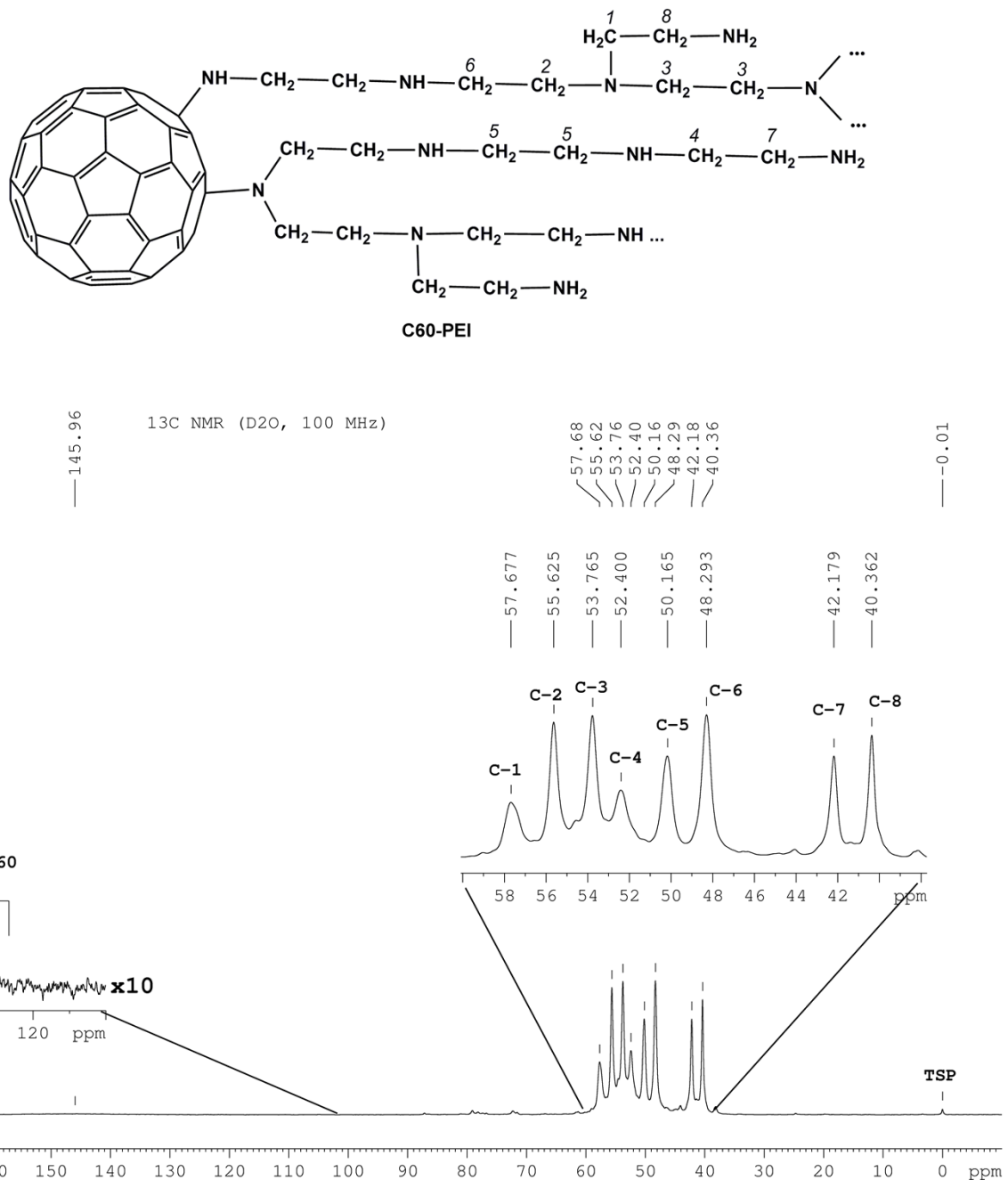


Figure SI-9. ^{13}C -NMR spectrum of the C60-PEI conjugate.

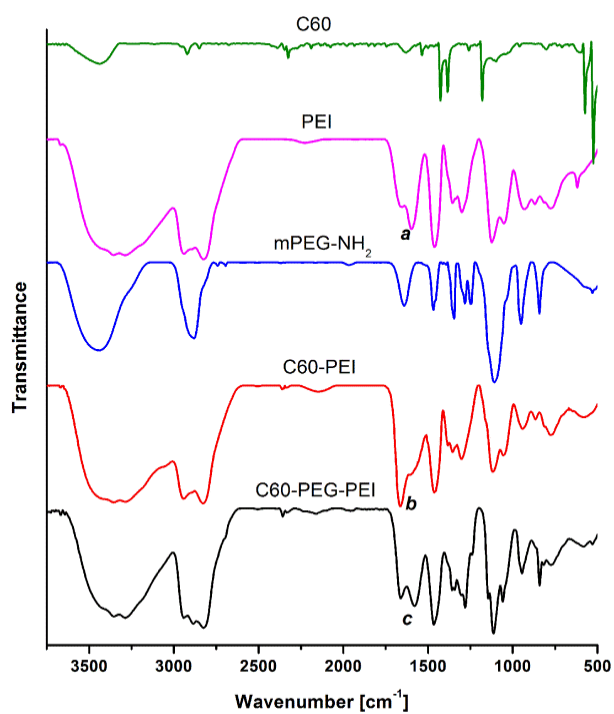


Figure SI-10. FT-IR spectra of the precursors and C60-based conjugates.

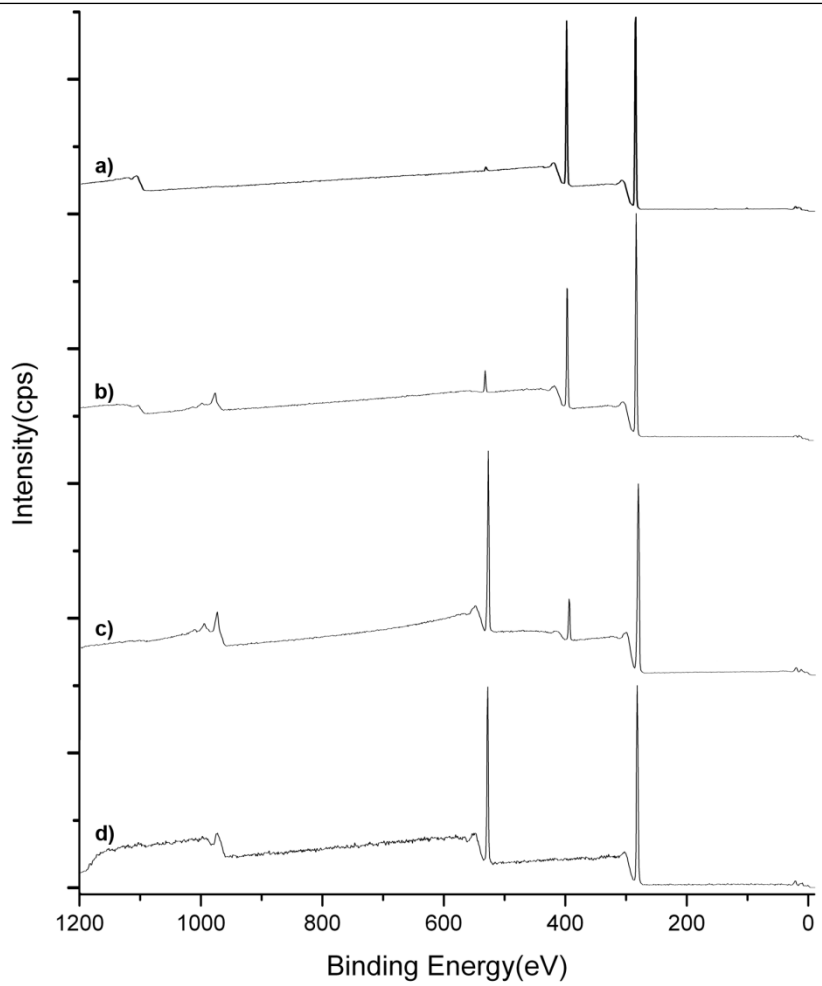


Figure SI-11. The wide scan XPS spectra of PEI (a), C60-PEI (b), C60-PEG-PEI (c), and mPEG-NH₂ (d).

Table SI-1. Elemental composition derived from wide scan XPS spectra.

Sample code	Mass concentration (%)		
	C	N	O
PEI	62.01	37.99	-
C60-PEI	65.98	34.02	-
C60-PEG-PEI	67.52	25.00	7.48
PEG	68.74	0.80	30.46

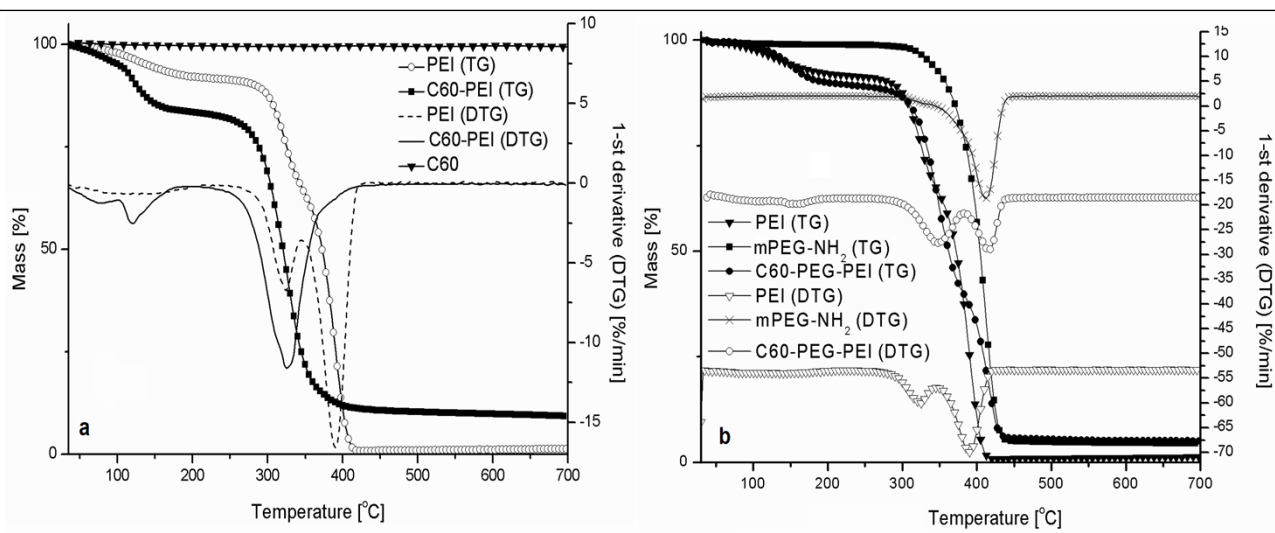


Figure SI-12. Comparative thermal characterization of PEI and PEG precursors, and of synthesized C60-PEI and C60-PEG-PEI conjugates.

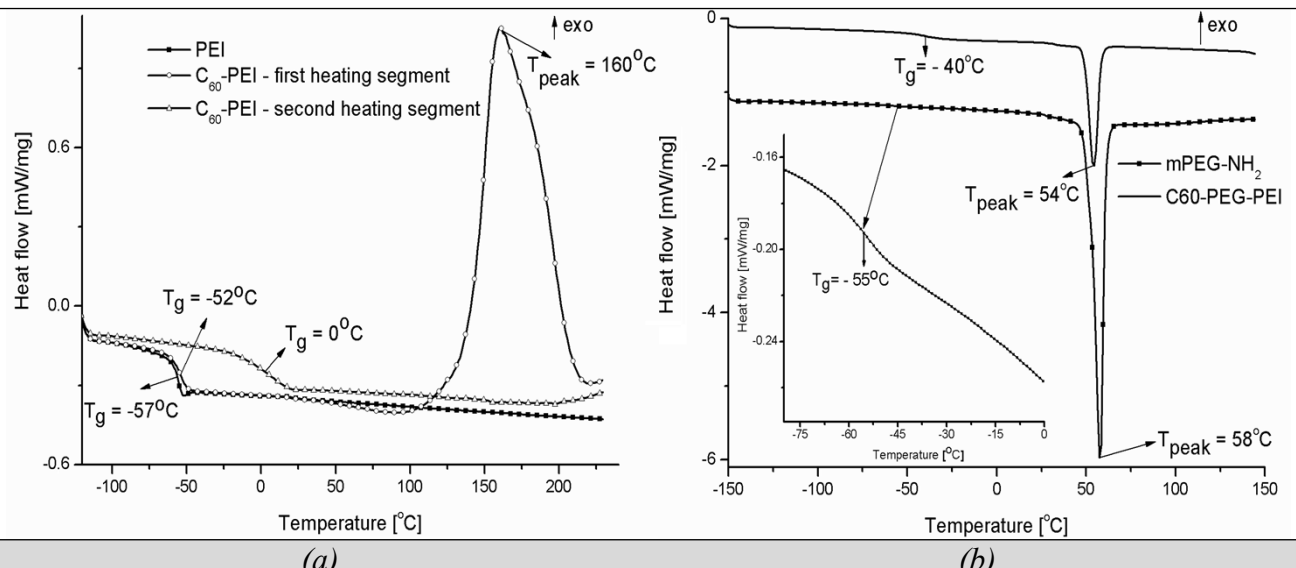


Figure SI-13. DSC heating curves of precursors and synthesized C60-based conjugates.